Radboud Repository

Radboud University Nijmegen

PDF hosted at the Radboud Repository of the Radboud University Nijmegen

The following full text is a publisher's version.

For additional information about this publication click this link.
http://hdl.handle.net/2066/34898

Please be advised that this information was generated on 2018-07-07 and may be subject to change.

physica status solidi a

phys. stat. sol. (a) **204**, No. 12, 4230–4240 (2007) / **DOI** 10.1002/pssa.200723324

Editor's Choice

Defect formation in GaN grown on vicinal 4H-SiC (0001) substrates

M. Rudziński[*, 1], **E. Jezierska**[2], **J. L. Weyher**[1, 3], **L. Macht**[1], **P. R. Hageman**[1], **J. Borysiuk**[2], **T. C. Rödle**[4], **H. F. F. Jos**[4], and **P. K. Larsen**[1]

[1] Applied Materials Science, Institute for Molecules and Materials, Radboud University, Toernooiveld 1, 6525 ED Nijmegen, The Netherlands
[2] Faculty of Materials Science & Engineering, Warsaw University of Technology, Woloska 141, 02-507 Warsaw, Poland
[3] Institute of High Pressure Physics, Polish Academy of Sciences, Sokolowska 29/37, 01-142 Warsaw, Poland
[4] NXP Semiconductors, Gerstweg 2, 6534 AE Nijmegen, The Netherlands

Received 6 June 2007, accepted 17 July 2007
Published online 1 October 2007

PACS 61.72.Ff, 61.14.Lj, 81.05.Ea, 81.15.Gh

We report a comparative study of wurtzite GaN epilayers prepared by Metal Organic Chemical Vapor Deposition on 4H-SiC substrates of orientation vicinal to the (0001) (misorientation 0°, 3.4°, and 8°). Structural analysis using X-ray diffraction, defect-selective etching methods, and (High Resolution-) Transmission Electron Microscopy provides direct evidence for a higher number of defects in GaN epilayers grown on the 8° misoriented substrate compared to the 3.4° and 0° misoriented substrates. We found strong differences in morphology of the GaN epilayers and in type and density of the defects formed during growth on both vicinal and nominally exact oriented SiC substrates. The formation of clusters of defects and the non-uniform distribution of strain, resulting in preferential cracking of the GaN films along the $[11\bar{2}0]$ direction, are both results of growth on misoriented substrates. Based on experimental results, the growth mechanism is discussed and a model explaining the defect formation is proposed.

© 2007 WILEY-VCH Verlag GmbH & Co. KGaA, Weinheim

1 Introduction

Group III nitride semiconductors are intensively investigated because of their favourable intrinsic properties for both electronic (high power, high frequency, high temperature) and optical devices. However, the absence of commercially available bulk nitride substrates implies the use of heteroepitaxial growth with host substrates having in general significantly smaller lattice parameters. The use of complex fabrication processes is then necessary to obtain good film quality. Two substrates are most often used, i.e. sapphire and SiC, of which silicon carbide (SiC) has the smallest lattice mismatch to GaN (~3.8%). Moreover, the high thermal conductivity and the availability of conducting as well as semi-insulating substrates makes SiC attractive for the realization of both transistors [1] and optoelectronic devices [2]. To increase the efficiency of these devices, a great deal of effort is being invested in the growth of high quality epitaxial layers. As a consequence, studies of AlN and GaN growth mechanisms on SiC gained increasing interest

* Corresponding author: e-mail: mariusz.rudzinski@gmail.com, Tel.: +31 24 3653158, Fax: +31 24 3652314

WILEY InterScience® DISCOVER SOMETHING GREAT

© 2007 WILEY-VCH Verlag GmbH & Co. KGaA, Weinheim

Editor's Choice

over the last few years [3, 4]. In Molecular Beam Epitaxy (MBE) growth of GaN epilayers, the use of a vicinal SiC substrate under optimized step-flow growth conditions has been a popular strategy to reduce the density of threading screw dislocation [5]. In the case of homoepitaxy of SiC by Chemical Vapor Deposition (CVD), the use of off-oriented instead of exact-oriented SiC substrates resulted in an improved surface smoothness [6]. Along these views, we discuss in this work the possibility of using (0001)-misoriented 4H-SiC substrates for the growth of GaN layers by Metal Organic Chemical Vapor Deposition (MOCVD). We report strong differences in GaN morphology and in type and density of defects formed during growth on both vicinal and nominally exact oriented SiC substrates, and we discuss the structural properties of the layers.

2 Experimental

The GaN epilayers were deposited on quarters of 4H-SIC wafers in the MOCVD reactor. In the MOCVD process trimethylgallium (TMG), trimethylaluminium (TMA), and ammonia (NH_3) were used as precursors and H_2 as the carrier gas. A 120 nm thick AlGaN nucleation layer with a low Al content (≅ 1 at%) [7] was grown at identical conditions as the GaN layer, being 1170 °C at 50 mbar pressure. The growth time was set to obtain about 1.8 μm GaN for the layers discussed in this paper. Three sets of 4H-SiC substrates were used, namely on-axis, 3.4° and 8° misoriented in the $[11\bar{2}0]$ direction. Samples #1, #2, #3 were grown at the same growth run. Some dedicated samples were grown with a thickness of only 0.75 μm in order to obtain crack-free samples. To check the structural quality of all epilayers, the samples have been examined by X-ray rocking curve mode using a Bruker D8 Discovery X-ray diffractometer with a Cu target (λ = 1.54060 Å) and a 4-bounce monochromator Ge (022). From all samples, small pieces were cut to perform defect-selective etching using molten eutectic mixture of KOH–NaOH (E) with 10% of MgO powder (E + M) [8]. Additionally, some samples were also subjected to photo-etching in a stirred KOH solution (0.004 molar) at room temperature using UV illumination provided by a 450 W Xe lamp. A 100 nm thick Ti layer was used to assure photocurrent conduction [9]. In this way the defect density and distribution over the wafer was revealed. The surface morphology before and after (E + M) and photo-etching was examined using Differential Interference Contrast (DIC) optical microscopy, Scanning Electron Microscopy (SEM), and Atomic Force Microscopy (AFM, Digital Instrument Nanoscope Dimension 3100 SPM). Cross-sectional structural characterizations were performed using high-resolution (HR) and conventional Transmission Electron Microscopy (TEM) using a JEM 3010 (300 kV) Jeol microscope equipped with a Gatan SS CCD camera. Cross-sectional, electron transparent foils were prepared by Ar-ion milling using a Gatan Precision Ion Polishing System (PIPS).

3 Results and discussion

3.1 Observations

Examination of the morphology of samples using DIC optical microscopy, AFM, and SEM revealed that crack-free GaN epilayers of 1.8 μm thickness can be grown only on the on-axis substrates using the described growth conditions and a HT-AlGaN nucleation layer. In the case of the misoriented substrates, cracks are always visible over the whole surface but are of different density and distribution depending on the degree of misorientation. All cracks in the GaN epilayers grown on 8° misoriented substrates are parallel to the $[11\bar{2}0]$ direction. The 3.4° misoriented substrates show, when compared to the 8° misoriented substrate, a reduced crack density with a different orientation, viz. $[2\bar{1}\bar{1}0]$, $[11\bar{2}0]$ and $[\bar{1}2\bar{1}0]$ directions [10]. No overgrown cracks can be found on the epilayers, therefore it must be concluded that these cracks are formed during cooling down due to thermal expansion coefficient differences between GaN and SiC.

Apart from the increased density of cracks, the epilayers grown on misoriented substrates (8° and 3.4° off-axis samples) show also an increased dislocation density as was observed by TEM. Figure 1 shows cross sectional TEM images with a projection close to the $[11\bar{2}0]$ orientation with a slight tilt in order to

 © 2007 WILEY-VCH Verlag GmbH & Co. KGaA, Weinheim

physica status solidi a

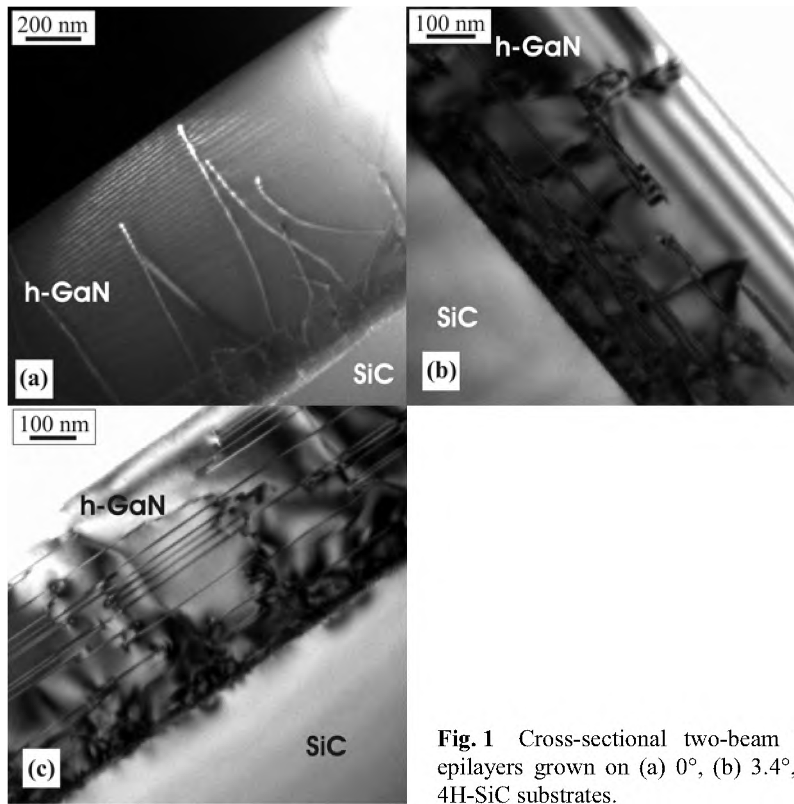

Fig. 1 Cross-sectional two-beam TEM images of GaN epilayers grown on (a) 0°, (b) 3.4°, and (c) 8° misoriented 4H-SiC substrates.

achieve a two-beam condition which enhances the contrast between stacking faults (SF) and dislocations. Due to the low Al fraction in the AlGaN nucleation layer (1–2%) and the high number of defects at the GaN/AlGaN interface, it was not possible to distinguish the AlGaN nucleation layer on the presented TEM images. Basal plane stacking faults (BPSF), prismatic stacking faults, and dislocations are visible in all samples. However, many of these defects are terminated at a certain depth in the GaN layer grown on the on-axis substrate (Fig. 1a) while extended arrangements of basal plain and prismatic stacking

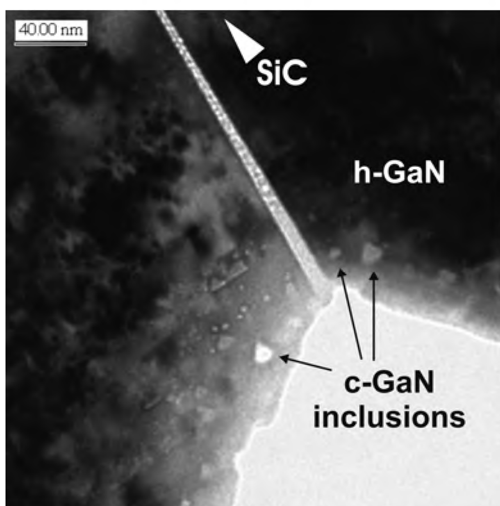

Fig. 2 Cross-sectional TEM micrograph for sample with 8° misorientation revealing c-GaN inclusions.

© 2007 WILEY-VCH Verlag GmbH & Co. KGaA, Weinheim

faults and dislocations (threading and stair-rod dislocations) were found throughout the whole GaN film grown on off-axis samples, even in the upper part of the layer. High numbers of basal and prismatic stacking faults are visible, especially in 8° off-axis material (Fig. 1c).

Additionally, c-GaN inclusions were found in the 8° misoriented layer as colonies of triangular pyramids with the tip of triangle towards the SiC substrate (Fig. 2). The presence of c-GaN inclusions were confirmed by micro-Raman spectroscopy [11]. The size of c-GaN inclusions is in the range 2–16 nm with an average lateral diameter near 5 nm.

A high resolution cross-sectional TEM image of a c-GaN inclusion embedded in the h-GaN epilayer is shown in Fig. 3. The flat interface of c-GaN inclusion is parallel to the basal plane of the h-GaN matrix. Inside the inclusion the symmetry of the structure is different from the surrounding matrix and a change in the stacking sequence of planes is visible. Instead of the ABAB stacking sequence, characteristic of hexagonal GaN, we can find the typical cubic phase ABCABC stacking sequence of atomic planes. Many groups reported the existence of cubic inclusions which has its origin in the low temperature nucleation layer or near the interface between the nucleation layer and the epitaxial layer [12–14].

In contrary, we have observed colonies of c-GaN inclusions across the whole GaN epilayer. Furthermore, it was observed that the surrounding area of the colonies of c-GaN inclusions has a reduced number of defects such as threading dislocation and stacking faults, which might suggest a local relaxation of h-GaN. The reason for the c-GaN formation is not entirely clear at present. The V/III ratio [15, 16], growth temperature [17], and substrate treatment [18] are factors which have often been discussed in the literature as a requirement for the stabilization of cubic GaN. Xie et al. [19] observed anisotropic growth behavior of GaN (0001) thin films by changing the growth temperature. Lowering the temperature changed the growth mode from step-flow to two-dimensional nucleation which resulted in a mixture of hexagonal and cubic oriented islands [19]. In our case identical growth conditions have been used, therefore it is obvious that the appearance of cubic GaN inclusions can not be assigned to difference in the growth conditions. However, directional step growth on vicinal substrates and continuation of the stacking order of atoms from the substrate can explain formation of SF and cubic inclusions. This fact can only explain existence of c-GaN in the area close to the SiC substrate but not the presence of these defects across the whole GaN layer. Nevertheless it is possible that BPSF formed in GaN grown on vicinal substrates (Fig. 1) carry information of the different order of atoms to the upper parts of GaN film and locally builds up the c-GaN inclusions. However, we could not find any explanation why and where BPSF could be transformed locally to c-GaN.

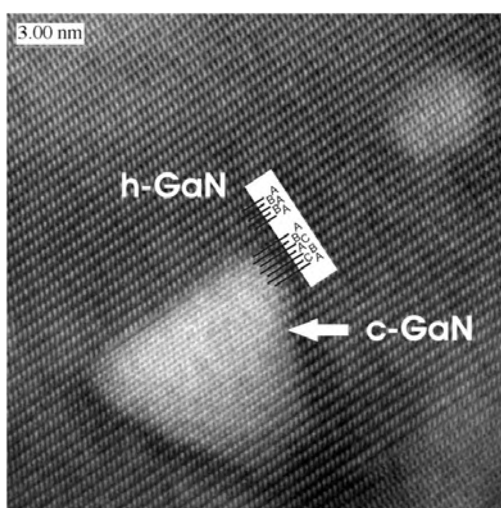

Fig. 3 Cross-sectional HRTEM image for sample with 8° misorientation revealing cubic GaN inclusions and its different sequence of closed packing planes compared to hexagonal GaN matrix.

 © 2007 WILEY-VCH Verlag GmbH & Co. KGaA, Weinheim

3.2 Defect distribution

To confirm the conclusions regarding the dislocation density in the different samples as was observed by TEM, X-ray rocking curve measurements were performed. In GaN layers, screw dislocations result in a tilt of lattice planes which can be detected by rocking curve measurements using symmetrical X-ray reflections (although it is not the only cause of broadening of the peak). On the other hand, edge-type dislocations introduce a twist of the in-plain lattice. To have access to this information, it is useful to perform ω-scans of a-symmetrical reflections. The full width at half maximum (FWHM) does not directly correspond to the twist [20], but a comparison between the samples is a good indication of their quality. X-ray rocking curve measurements on these samples, which were previously reported [10], showed that the structural quality of the GaN epilayer is worse for larger miscut angles. In particular, the FWHM of the asymmetric $(10\bar{1}5)$ peak increased significantly. Additional X-ray rocking curve measurements, both from symmetric and asymmetric planes, were performed using two different directions of the incoming X-ray beam ($[\bar{1}\bar{1}20]$ and $[1\bar{1}00]$). The results are presented in Table 1. The samples #1, #2, and #3 were, as mentioned, grown under identical conditions. They show very clearly a strongly increased FWHM for the misoriented samples. For off-axis samples (#2, #3 and #4), significant differences between the FWHM of the same (0002) plane but measured from two different beam directions, $[\bar{1}\bar{1}20]$, and $[1\bar{1}00]$ are observed, which can be an indication of: (1) a non uniform distribution of strain, and/or (2) a non uniform defect distribution, and also (3) the presence of different types and orientations of defects in the GaN films when compared to samples grown on the exact oriented substrates.

In the following part of the paper several experiments are described to elucidate if a non-uniform distribution of defects or the presence of different type of defects may be the origin for the observed X-ray results.

In order to check if the defect distribution is non uniform and to look for the presence of different types and orientations of defects in the GaN films, defect selective etching was performed and afterwards the samples were examined using SEM and tapping mode AFM. Selective etching of the GaN layer grown on the exact oriented substrate (Fig. 4a and b) yielded patterns of hexagonal pits, occurring in three grades of size representing the presence of edge, screw, and mixed dislocations. The small asymmetry in the shape of the etch pits formed on layers grown on the 3.4° misoriented substrate (Fig. 4c and d) reflects the difference between the direction of the dislocations line and the misorientation. Most of the typical threading dislocations created in the GaN layer during growth are in the [0001] direction. Therefore these defects will not be perpendicular to the GaN surface in layers grown on mis-cut substrates. Following this reasoning it is expected that when the misorientation of the substrate increases the tilt of the threading dislocations vs. the etched surface also increases and thus enlarges the asymmetry of the hexagonal pits. However, for the substrate with the 8° misorientation so-called arrow-like pits were formed instead of the hexagonal shape pits (Fig. 4e and f).

This unexpected form of the pits on the 8° misoriented sample is accompanied by a low apparent dislocation density. The dislocation densities for 8° off-axis, 3.4° off-axis, and on-axis samples, deduced from 4 × 5 μm² SEM images, reported before [10] were 6×10^8 (based on the assumption that one arrow-

Table 1 FWHM of the symmetric (0002) and asymmetric $(01\bar{1}4)$ X-ray rocking curves, of GaN grown on on-axis, 3.4° and 8° off-axis 4H-SiC substrates.

ID	misorientation	d_{GaN} [μm]	FWHM (0002)[1] [arcsec]	FWHM (0002)[2] [arcsec]	FWHM $(01\bar{1}4)$ [arcsec]	FWHM $(\bar{1}104)$ [arcsec]
#1	0°	1.80	137	139	151	132
#2	3.4°	1.65	159	191	169	195
#3	8°	1.65	209	537	566	634
#4	8°	0.75	234	508	–	695
#5	0°	0.75	270	266	–	194

(1) X-ray direction of incoming beam $[\bar{1}\bar{1}20]$, (2) X-ray direction of incoming beam $[1\bar{1}00]$.

© 2007 WILEY-VCH Verlag GmbH & Co. KGaA, Weinheim

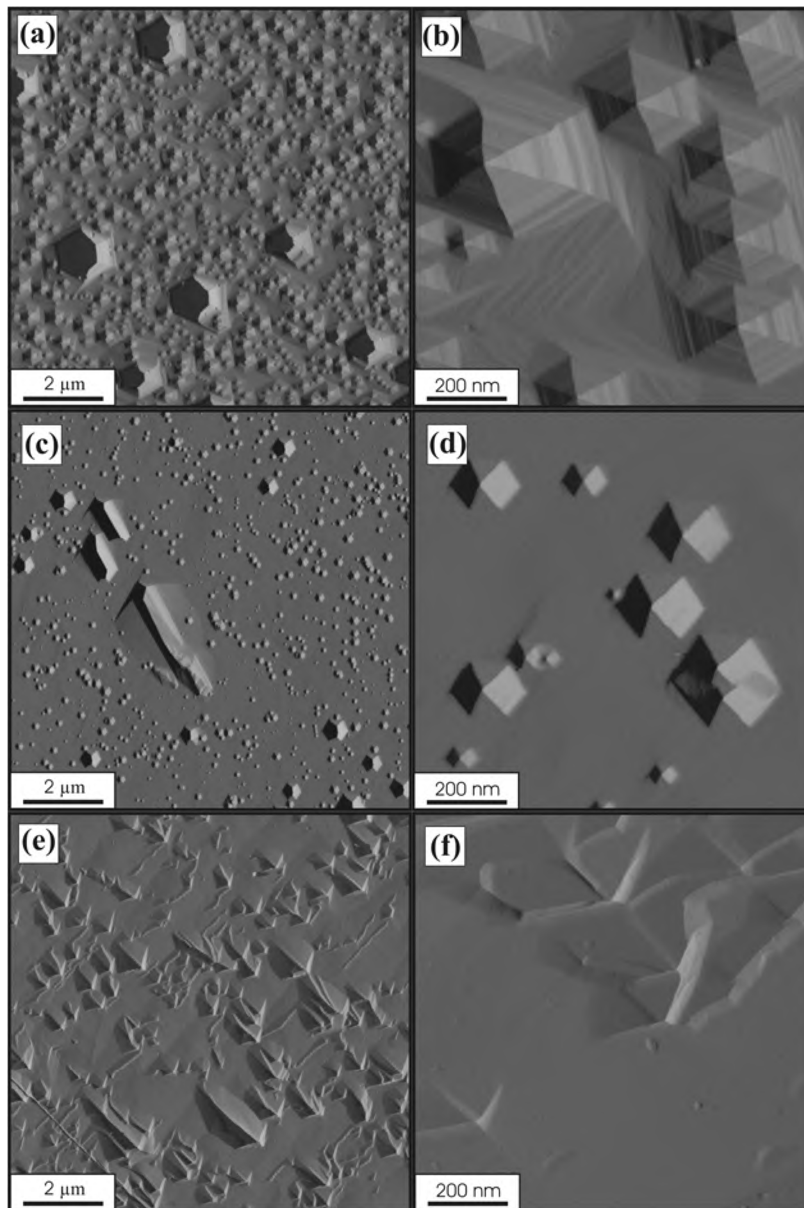

Fig. 4 AFM images of defects after etching in molten (E + M) of GaN epilayers grown on: (a), (b) an exact oriented, (c), (d) 3.4° misoriented and (e), (f) 8° misoriented 4H-SiC substrates.

like pit represents one dislocation), 9×10^{8}, and 2×10^{9} cm ^{2}, respectively. This is inconsistent with the conclusions drawn from X-ray and cross-sectional TEM measurements.

Photo-etching can be employed to reveal extended structural defects in n-type GaN films [9], and may therefore give insight in the formation of the arrow-like pits and explain the low dislocation density in the GaN layers grown on 8° misoriented substrates. Photo-etching of the crack free samples with 0° and 8° off-orientation was performed to be able to elucidate the influence of the misorientation on the defect formation. We expected that the dislocations, which were revealed after (E + M) etching as arrow-like pits, consisted of a number of threading dislocations which PEC etching can resolve. Photo-etching of

 © 2007 WILEY-VCH Verlag GmbH & Co. KGaA, Weinheim

physica status solidi a

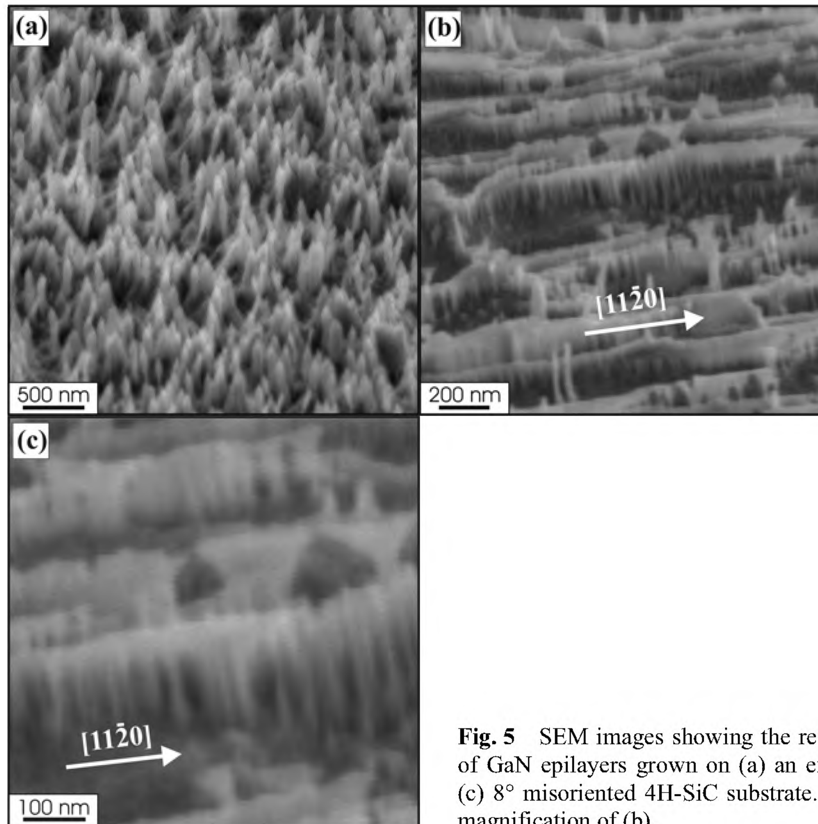

Fig. 5 SEM images showing the results of photo-etching of GaN epilayers grown on (a) an exact oriented and (b), (c) 8° misoriented 4H-SiC substrate. Image (c) is a larger magnification of (b).

the exact oriented sample (Fig. 5a) reveals the dislocations in the form of whiskers, the density (2.5×10^9 cm^{-2}) of which is a direct measure of the density of dislocations in the GaN epitaxial layers as was demonstrated by calibration of the etch features with cross-sectiona [19, 21] and plan-view [22] transmission electron microscopy. However, the GaN layer deposited on the 8° off-orientated substrate shows elongated features instead of whiskers (Fig. 5b and c). During photo-etching GaN does not etch when it is depleted of holes due to recombination at defects [23]. This implies that the elongated structures, visible in Fig. 5b and c, consist of material which contains a lot of recombination centers for the holes that are created by UV light. Due to the facts that these structures are only visible in etched GaN layers grown on the 8° misoriented substrates and that their orientation exactly match the orientation of the arrow-like pits, which are revealed after defect selective etching using molten (E + M) (Fig. 6a), it is suggests that we are dealing with the same type of defects. A larger magnification of the elongated features reveals that they consist of a high number of very closely spaced columnar defects (Fig. 5c). Clearly these are rows of threading edge dislocations, which could not be identified after defect selective etching using molten (E + M) because of overlapping of the small etch pits. The assumption that the elongated defects consists of mainly threading edge dislocations was supported by a molten (E + M) etching experiment in conditions which revealed only screw type dislocations. The activation energy for the formation of pits on edge dislocations is larger than that for dislocations with a screw component [24]. Therefore, at lower etching temperature (240 °C) only dislocations with a screw component are revealed. Etching at 240 °C (Fig. 6b and d) instead of 400 °C (Fig. 6a, and c) resulted in a considerably lower number of etch pits for both 8° off-cut and on-axis grown samples. This leads to the conclusion that most of the arrow-like pits are formed on edge dislocations. The assumption that one arrow-like pit represents one dislocation as was proposed in our previous paper [10] was incorrect; the number of defects calculated as 6×10^8 cm^{-2} will be two orders of magnitude higher, approximately 3×10^{10} cm^{-2}. Therefore, as

© 2007 WILEY-VCH Verlag GmbH & Co. KGaA, Weinheim

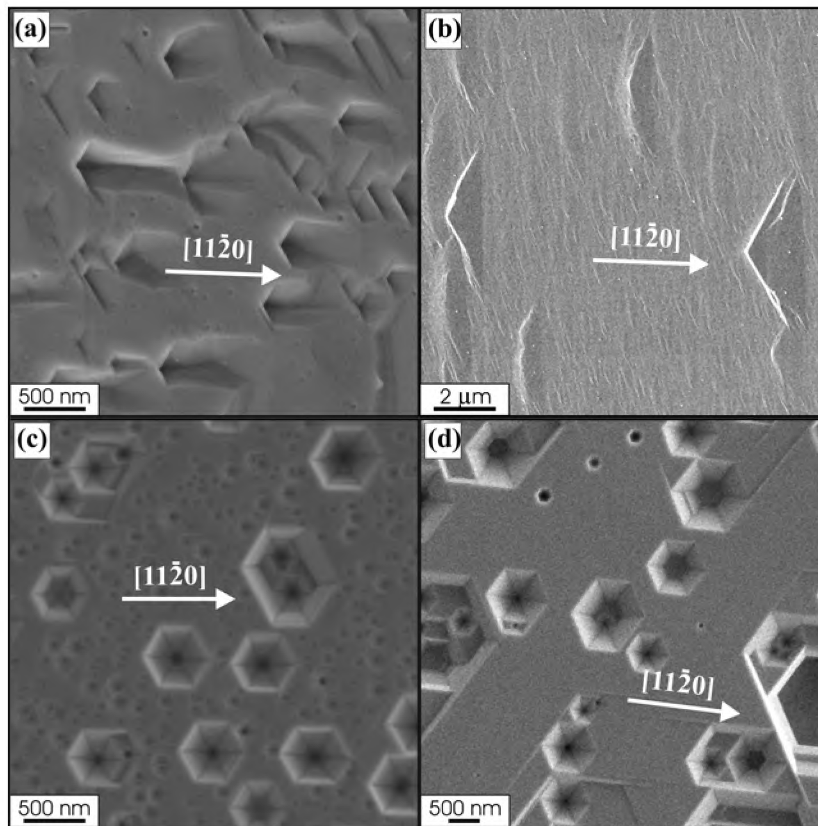

Fig. 6 SEM images showing the results of defect selective etching in molten (E + M) of GaN epilayers grown on (a), (b) 8° misoriented, and (c), (d) an exact oriented 4H-SiC substrate. Samples (a), (c) were etched at 400 °C for 2 minutes, and (b), (d) were etched at 240 °C for 10 minutes.

expected and shown in the presented TEM experiments, the dislocation density for the 8° off-axis sample is higher compared to 3.4° and 0° oriented samples.

From these results it can be concluded that the formation of the arrow-like pits in the 8° misoriented samples can be a cause for the observed X-ray results.

3.3 Formation of arrow-like defects

In Fig. 7 a model is proposed which explain the formation of walls of edge-type dislocations. The surface of the SiC substrates consists of (0001) flat terraces and steps. On the exact-oriented (0001) faces, epitaxial growth initially takes place on the terraces, because the surface step density is low and the terraces are sufficiently vast compared with the migration length of atoms on the surface [25]. On the misoriented substrates in the [11$\bar{2}$0] direction, micro-steps are induced on the surface and they are perpendicular to [11$\bar{2}$0] direction (or, aligned along [1$\bar{1}$00] direction), see Fig. 7a. The micro-step height is expected to be of a monolayer height of 4H-SiC (0.25 nm). Therefore, the calculated length of the terraces for 8°-off substrates is around 1.8 nm for the steps. If the steps are a multiple of a monolayer height, the terrace length increases. Since the step density is high and the terraces are not very long, incorporation of atoms at step edges dominates and nucleation centers on the terraces are greatly suppressed so lateral growth (step flow growth) from the steps takes place (Fig. 7b). In this case, the growth direction is determined by the presence of well ordered steps. Due to the orientation mismatch at the grain boundaries between the different AlGaN nuclei, edge dislocations are formed like it is schematically presented in Fig. 7c.

 © 2007 WILEY-VCH Verlag GmbH & Co. KGaA, Weinheim

physica status solidi a

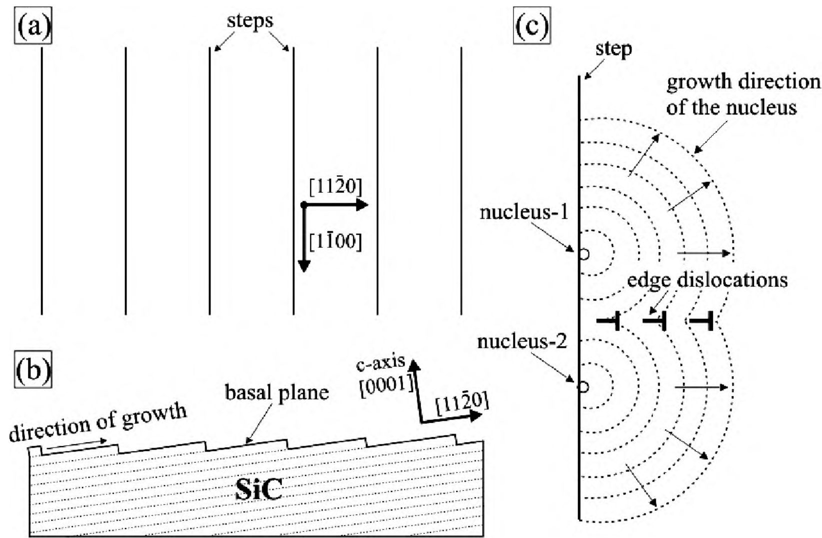

Fig. 7 Planar (a) and cross-sectional (b) schematic diagrams illustrating the configuration of steps and step flow growth on the surface of an off-axis SiC substrates, and (c) schematic diagram illustrating the formation of edge dislocations during AlGaN/GaN growth.

During GaN growth these defects propagate into GaN film. The misfit between the nucleuses orientation is about 1.8°, which was calculated from the average distance between the dislocations (~20 nm) forming elongated features (Fig. 5c), using the formula given by D. Hull and D. J. Bacon [26].

It was already mentioned that, on the on-axis SiC the steps are more random, less dense and terraces length is larger when compared to the 8° off-axis substrates. Therefore nucleation on on-axis substrates is random and due to the fact that the growth direction is not determined by the step orientation, the lateral growth is faster. This can explain growth rate difference which was found to be 1.8 µm/h and 1.65 µm/h as measured for on axis and off-axis samples, respectively (grown in the same growth run).

On 8° off-cut substrates, the lateral growth is initiated on the steps, inheriting the stacking order of atoms from the substrate. In the case of homoepitaxial growth (SiC on SiC), high quality and very smooth layers were observed [27]. However, during heteroepitaxy the step height is determined by the SiC substrate and not by the GaN layer and the step height does not correspond to the unit cell of GaN. One monolayer of GaN is 2.59 Å in contrast to 2.51 Å of 4H-SiC (c_{GaN} = 5.185 Å, c_{SiC} = 10.05 Å). As a

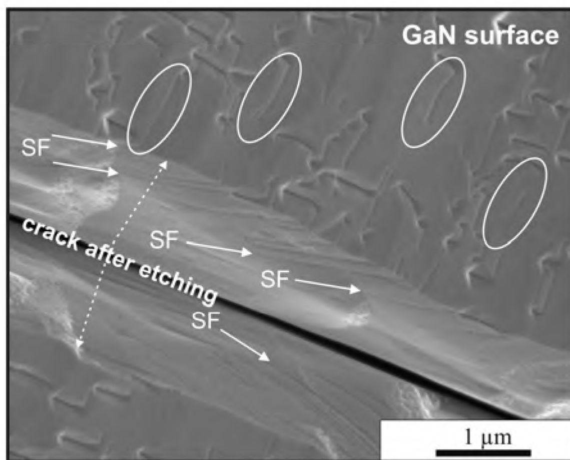

Fig. 8 SEM image for sample with 8° misorientation after defect selective etching, revealing the orientation of basal plain stacking faults (BPSFs) and arrow-like pits representing edge dislocations. At the slope of the etched crack the BPSFs are marked by arrows; BPSFs on the GaN surface are marked by ellipses.

© 2007 WILEY-VCH Verlag GmbH & Co. KGaA, Weinheim

Editor's
Choice

consequence, not only for the *a*-plane but also in *c*-direction the large lattice mismatch of GaN and AlGaN to the substrate have to be considered, and therefore a higher number of defects are expected to be created. Recent structural characterization shows that the stacking faults and stacking mismatch boundaries (SMB) defects in GaN epilayers really originate from the steps on sapphire and SiC surfaces [28]. Misfit in *c*-direction between AlGaN and SiC is a driving force for the formation of BPSFs, which were revealed by TEM (Fig. 1). It is important to point out that in the 8° misoriented sample, the BPSFs are not parallel to the surface of the sample. The orientation of the BPSFs is not visible on the TEM images because the cross-section of the specimens has been cut along the $(11\bar{2}0)$ plane. The main reason for preparing the thin foil in this orientation was to prevent the destruction of the specimens because of the cracks along the $[11\bar{2}0]$ direction. For this reason, additional SEM inspections have been performed on each of the samples after defect selective etching. Only on the 8° misoriented sample the BPSFs have reached the GaN surface, as shown in Fig. 8.

3.4 Crack formation

The formation of cracks can be explained by the presence of non uniformly distributed strain. Recently, Huang et al. [29] found that unpaired geometrical partial misfit dislocations (GPMDs) are formed along the step of the AlN/6H-SiC interface to improve the stacking sequence between 2H and 6H structures for misoriented substrates. This strain relaxation mechanism must be present at the AlGaN/SiC interface with a 2H/4H stacking structure in this case. For this system, the proportion of steps corresponding to GPMDs is 1/2 [29] since the number of cubic sites is 1/2 in the ABAC stacking sequence (one cubic site is defined as the B bilayer in the ABC sequence and one hexagonal site is defined as the B layer in the ABA sequence). This mechanism takes place during the step-flow growth, giving GPMDs lines along $[1\bar{1}00]$ axis and so, relaxing the $[11\bar{2}0]$ strains. Huang et al. [29], on the basis of geometrical considerations (miscut angle and stacking sequence), argue that the number of GPMDs can be controlled, relaxing the $[11\bar{2}0]$ strains. This explains the difference between the the 3.4° and 8° misoriented samples. During the growth and prior to cooling, more GPMDs are formed along the $[1\bar{1}00]$ axis in samples grown on 8° misoriented substrates than in samples grown on 3.4° misoriented ones, limiting more efficiently the $[11\bar{2}0]$ strain. Then, during cooling down after growth, the thermal expansion coefficient difference between GaN and SiC puts the GaN epilayer under tensile in-plane strain, creating some cracks [30]. So, during cooling down, the thermal expansion coefficient difference induces a high tensile strain along the $[1\bar{1}00]$ direction for the two miscut angles. This would also explain the formation of cracks along the $[11\bar{2}0]$ direction perpendicular to the $[1\bar{1}00]$ direction. The $[11\bar{2}0]$ strain could be highly relaxed by the GPMDs for the 8° misoriented samples and not so much for 3.4° misoriented samples, explaining the formation of additional cracks in the $[2\bar{1}\bar{1}0]$ and $[\bar{1}2\bar{1}0]$ directions (not perpendicular to the $[1\bar{1}00]$ axis) for this sample.

To summarize, for the off-cut samples (3.4° and 8°), the strain relaxation seems to be mainly governed by two successive steps:

(i) Creation of the edge dislocation walls along the $[11\bar{2}0]$ axis, GPMDs along the $[1\bar{1}00]$ axis [29], basal plane stacking faults, prismatic stacking faults, and stair rod dislocations [31] during the step-flow growth due to the misorientation of the substrate.

(ii) Creation of cracks along the $[11\bar{2}0]$ direction (and also along $[2\bar{1}\bar{1}0]$ and $[\bar{1}2\bar{1}0]$ for the samples 3.4° misoriented) during the cooling process due to the difference of the thermal expansion coefficients and in particular directions to minimize the residual stress.

4 Conclusions

Variations in quality of the GaN layer have been demonstrated when grown on differently oriented 4H-SiC substrates. Similar defects including stacking faults on basal and prismatic planes, complexes of extended stacking faults, and dislocations (threading and stair-rod dislocations) were found for all samples. The density of these defects increases with the substrate miscut.

Elongated defects and colonies of c-GaN inclusions were found only in the samples grown on 8° off-cut substrates. Unusual formation of the high number of tightly packed rows of dislocations induces not

 © 2007 WILEY-VCH Verlag GmbH & Co. KGaA, Weinheim

uniform relaxation of the material; therefore only $[11\bar{2}0]$ directed cracks are created during cooling down the GaN film after growth.

The mechanism of the formation of these defects is not fully understood yet, nevertheless it is suggested that difference in the growth mechanism of GaN due to substrate misorientation is responsible for this effect. We presented tentative model which explains formation of rows of threading edge dislocations and directional cracking.

Acknowledgements The financial support of M. Rudziński by NXP, formerly Philips Semiconductors B.V. Nijmegen is gratefully acknowledged. One of the authors (JLW) acknowledged the financial support of the Netherlands Foundation for Technical Research (STW).

References

[1] Y.-F. Wu, A. Saxler, M. Moore, R. P. Smith, S. Sheppard, P. M. Chavarkar, T. Wisleder, U. K. Mishra, and P. Parikh, IEEE Electron Device Lett. **25**, 117 (2004).
[2] M. Iwaya, H. Kasugai, T. Kawashima, K. Iida, A. Honshio, Y. Miyake, S. Kamiyama, H. Amano, and I. Akasaki, Thin Solid Films, in press.
[3] S. Yamada, J. I. Kato, S. Tanaka, I. Suemune, A. Avramescu, Y. Aoyagi, N. Teraguchi, and A. Suzuki, Appl. Phys. Lett. **78**, 3612 (2001).
[4] C. D. Lee, A. Sagar, R. M. Feenstra, C. K. Inoki, T. S. Kuan, W. L. Sarney, and L. Salamanca-Riba, Appl. Phys. Lett. **79**, 3428 (2001).
[5] M. H. Xie, L. X. Zheng, S. H. Cheung, Y. F. Ng, H. Wu, S. Y. Tong, and N. Ohtani, Appl. Phys. Lett. **77**, 1105 (2000).
[6] H. S. Tong, J. T. Glass, and R. F. Davis, J. Appl. Phys. **64**, 2673 (1988).
[7] H. Lachrèche, P. Vennéguès, M. Vaille, B. Beaumont, M. Laügt, P. Lorenzini, and P. Gibart, Semicond. Sci. Technol. **14**, 33 (1999).
[8] G. Kamler, J. L. Weyher, I. Grzegory, J. Jezierska, and T. Wosinski, J. Cryst. Growth **246**, 21 (2002).
[9] C. Youtsey, R. T. Romano, and I. Adesida, Appl. Phys. Lett. **73**, 797 (1998).
[10] M. Rudziński, P. R. Hageman, A. P. Grzegorczyk, L. Macht, J. Pernot, T. C. Rödle, H. F. F. Jos, and P. K. Larsen, phys. stat. sol. (c) **2**, 2141 (2005).
[11] J. Pernot, E. Bustarret, M. Rudziński, P. R. Hageman, and P. K. Larsen, J. Appl. Phys. **101**, 1 (2007).
[12] S. Strauf, P. Michler, J. Gutowski, H. Selke, U. Birkle, S. Einfeldt, and D. Hommel, J. Cryst. Growth **189**, 682 (1998).
[13] D. J. Smith, D. Chandrasekhar, B. Sverdlov, A. Botchkarev, A. Salvador, and H. Morkoc, Appl. Phys. Lett. **67**, 1830 (1995).
[14] X. H. Wu, P. Fini, E. J. Tarsa, B. Heying, S. Keller, U. K. Mishra, S. P. DenBaars, and J. S. Speck, J. Cryst. Growth **189**, 231 (1998).
[15] T. Kurobe, Y. Sekiguchi, J. Suda, M. Yoshimoto, and H. Matsunami, Appl. Phys. Lett. **73**, 2305 (1998).
[16] H. Tsuchiya, K. Sunaba, S. Yonemura, T. Suemasu, and F. Hasegawa, Jpn. J. Appl. Phys. **36**, L1 (1997).
[17] R. Armitage, K. Nishizono, J. Suda, and T. Kimoto, J. Cryst. Growth **284**, 369 (2005).
[18] J. Suda, T. Kurobe, and H. Matsunami, J. Cryst. Growth **201**, 437 (1999).
[19] M. H. Xie, S. M. Seutter, W. K. Zhu, L. X. Zheng, H. Wu, and S. Y. Tong, Phys. Rev. Lett. **82**, 2749 (1999).
[20] Y. J. Sun, O. Brandt, T. Y. Liu, A. Trampert, K. H. Ploog, J. Blasing, and A. Krost, Appl. Phys. Lett. **81**, 4928 (2002).
[21] J. L. Weyher, F. D. Tichelaar, H. W. Zandbergen, L. Macht, and P. R. Hageman, J. Appl. Phys. **90**, 6105 (2001).
[22] C. Youtsey, R. T. Romano, R. J. Molnar, and I. Adesida, Appl. Phys. Lett. **74**, 3537 (1999).
[23] J. L. Weyher and L. Macht, Eur. Phys. J. Appl. Phys. **27**, 37 (2004).
[24] J. L. Weyher, Superlattices Microstruct., in press.
[25] T. Ueda, H. Nishino, and H. Matsunami, J. Cryst. Growth **104**, 695 (1990).
[26] D. Hull and D. J. Bacon, Introduction to Dislocations (Pergamon Press, 1984), p. 27.
[27] B. E. Landini and G. R. Brande, Appl. Phys. Lett. **74**, 2632 (1999).
[28] P. Ruterana, B. Barbaray, A. Bere, P. Vermaut, A. Hairie, E. Paumier, G. Nouet, A. Salvador, A. Botchkarev, and H. Morkoc, Phys. Rev. B **59**, 15917 (1999).
[29] X. R. Huang, J. Bai, M. Dudlay, B. Wagner, R. F. Davids, and Y. Zhu, Phys. Rev. Lett. **95**, 086101 (2005).
[30] J. Yamamoto et al., J. Cryst. Growth **189/190**, 193 (1998).
[31] J. Bai et al., J. Appl. Phys. **98**, 063510 (2005).

© 2007 WILEY-VCH Verlag GmbH & Co. KGaA, Weinheim